INTERNATIONAL JOURNAL FOR NUMERICAL METHODS IN FLUIDS, VOL. 6, 593–609 (1986)

MAGNETOHYDRODYNAMIC FLOW IN AN INFINITE CHANNEL

MÜNEVVER SEZGIN*

Department of Mathematics, Middle East Technical University, Ankara, Turkey

SUMMARY

The magnetohydrodynamic (MHD) flow of an incompressible, viscous, electrically conducting fluid in an infinite channel, under an applied magnetic field has been investigated. The MHD flow between two parallel walls is of considerable practical importance because of the utility of induction flowmeters. The walls of the channel are taken perpendicular to the magnetic field and one of them is insulated, the other is partly insulated, partly conducting. An analytical solution has been developed for the velocity field and magnetic field by reducing the problem to the solution of a Fredholm integral equation of the second kind, which has been solved numerically. Solutions have been obtained for Hartmann numbers M up to 200. All the infinite integrals obtained are transformed to finite integrals which contain modified Bessel functions of the second kind. So, the difficulties associated with the computation of infinite integrals with oscillating integrands which arise for large M have been avoided. It is found that, as M increases, boundary layers are formed near the non-conducting boundaries and in the interface region for both velocity and magnetic fields, and a stagnant region in front of the conducting boundary is developed for the velocity field. Selected graphs are given showing these behaviours.

KEY WORDS Infinite Channels MHD Flows

INTRODUCTION

The study of flows of conducting fluids in channels and ducts in the presence of a transverse magnetic field is important, owing to practical applications in magnetohydrodynamic (MHD) generators, pumps, accelerators and flowmeters. Various forms of the problem with different combinations of conducting and non-conducting walls have been considered by Shercliff,[1] Chang and Lundgren,[2] Gold,[3] Hunt[4] and others. Grinberg[5,6] has formulated the problem with perfectly conducting walls parallel to the applied field and non-conducting walls perpendicular to the field, and attempted an exact analysis using a Green's function method; but his result is incomplete. Later Hunt and Stewartson[7] and Chiang and Lundgren[8] used boundary layer methods to cast the same problem in the form of an integral equation. Lately Singh and Agarwal[9] followed Grinberg's solution procedure for the analytical part, but they solved the resulting singular integral equation numerically since it could not be solved easily. Hunt and Williams[10] investigated the MHD flow between two parallel non-conducting planes. Wenger[11] presented a variational formulation that gave exact solutions for the velocity profile and electric potential distribution for a duct with mixed boundary conditions, but the analysis was of a very complicated nature. Recently, Wu[12] and Singh and Lal[13–15] have applied finite element methods to solve steady and unsteady MHD channel flow problems for different wall conductances.

*Supported by The Scientific and Technical Research Council of Turkey.

0271–2091/86/090593–17$08.50

Received 30 September 1985
Revised 1 March 1986

In all of these studies except Wenger's,[11] each of the walls of the channels or ducts is either completely conductor or completely insulator, but not a mixture of two. In this paper, we are concerned with the flow of an incompressible, viscous, electrically conducting fluid through an infinite channel with an external magnetic field applied transverse to the flow. One of the boundaries (a wall of the infinite channel) perpendicular to the magnetic field is taken to be partly insulating and partly perfectly conducting. The problem is solved analytically by reducing it to the solution of a Fredholm integral equation of the second kind, which has been solved numerically. Several valid approximations have been made for large Hartmann numbers in the calculations of the kernel and the right hand side function of this integral equation. All the infinite integrals obtained in the solution are transformed to finite integrals which contain modified Bessel functions of the second kind. In this way, we have avoided the difficulties associated with the computation of infinite integrals with oscillating integrands, the convergence of which is affected for large values of the Hartmann number.

BASIC EQUATIONS

The fluid is taken as viscous, incompressible and having uniform electrical conductivity. It is driven down the infinite channel by means of a constant applied pressure gradient, and throughout its passage is subjected to a constant and uniform imposed magnetic field which is applied perpendicular to the direction of the flow. The magnetic field is also taken perpendicular to the boundary which is partly insulating and partly perfectly conducting. It is also assumed that the fluid motion is fully developed, steady and laminar.

The equations governing this problem have been derived by Shercliff[1] Dragos,[16] and others. The z-axis is taken as parallel to the fluid velocity and the x-axis is parallel to the imposed uniform magnetic field H_0 existing outside of the fluid. All physical quantities, except pressure, are assumed to be independent of z; the velocity vector has only a z-component, $V_z(x, y)$, and the magnetic field vector takes the form $\mathbf{H} = (H_0, 0, H_z(x, y))$. We also assume that displacement currents are negligible and that there is no net flow of current in the z-direction. So, the z-components of the equations are

$$\eta \nabla^2 H_z + H_0 \frac{\partial V_z}{\partial x} = 0, \tag{1}$$

$$\mu \nabla^2 V_z + \mu_e H_0 \frac{\partial H_z}{\partial x} = \frac{\partial P}{\partial z}, \tag{2}$$

where $\eta = (\sigma \mu_e)^{-1}$, which is known as magnetic diffusivity, σ and μ_e are electrical conductivity and magnetic permeability, respectively, μ is the coefficient of viscosity, P is the pressure of the fluid and ∇^2 is the two-dimensional Laplacian operator.

By using the relationship

$$\mathbf{B} = \mu_e \mathbf{H}, \tag{3}$$

where $\mathbf{B}$ is the magnetic induction vector, the equations (1) and (2) are written in terms of $\mathbf{B}$ as

$$\eta \nabla^2 B_z + B_0 \frac{\partial V_z}{\partial x} = 0, \tag{4}$$

$$\mu \nabla^2 V_z + \frac{B_0}{\mu_e} \frac{\partial B_z}{\partial x} = \frac{\partial P}{\partial z}, \tag{5}$$

where

$$B_0 = \mu_e H_0. \tag{6}$$

Introducing dimensionless variables

$$V = \frac{1}{v_0} V_z, \qquad B = \frac{(\sigma\mu)^{-1/2} B_z}{v_0 \mu_e}, \tag{7}$$

$$x' = \frac{x}{L_0}, \qquad y' = \frac{y}{L_0}, \tag{8}$$

where

$$v_0 = -L_0^2(\partial P/\partial z)/\mu \tag{9}$$

is the characteristic velocity (mean axis velocity) and L_0 is the characteristic length, we obtain the following equations for $V(x, y)$ and $B(x, y)$ (substituting $x' = x$, $y' = y$):

$$\nabla^2 B + M\frac{\partial V}{\partial x} = 0, \tag{10}$$

$$\nabla^2 V + M\frac{\partial B}{\partial x} = -1, \tag{11}$$

where

$$M = B_0 L_0 \sqrt{\sigma}/\sqrt{\mu} \tag{12}$$

is the Hartmann number.

Accordingly, the boundary conditions for equations (10) and (11) related to the configuration of the problem in Figure 1 are as follows:

$$V(0, y) = V(a, y) = 0, \qquad -\infty < y < \infty, \tag{13a}$$

$$B(a, y) = 0, \qquad -\infty < y < \infty, \tag{13b}$$

$$B(0, y) = 0, \qquad l < |y| < \infty, \tag{13c}$$

$$B_x(0, y) = 0, \qquad 0 \leqslant |y| < l. \tag{13d}$$

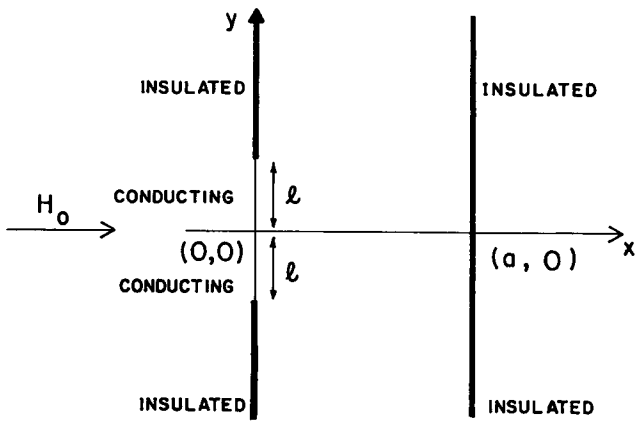

Figure 1.

ANALYTICAL SOLUTION

The method of solving the system (10) and (11) subject to boundary conditions (13) consists of splitting the solution into two parts as

$$\begin{pmatrix} V \\ B \end{pmatrix} = \begin{pmatrix} V_0 \\ B_0 \end{pmatrix} + \begin{pmatrix} V_1 \\ B_1 \end{pmatrix}. \tag{14}$$

Here '0' refers to the flow when the wall at $x = 0$ is insulated. We shall call it the primary flow. The solution corresponding to the suffix '1' gives the correction due to the conducting part of the boundary, and we shall designate the flow due to it as secondary flow. Thus, we have

$$\frac{d^2V_0}{dx^2} + M\frac{dB_0}{dx} = -1, \tag{15}$$

$$\frac{d^2B_0}{dx^2} + M\frac{dV_0}{dx} = 0, \tag{16}$$

with the boundary conditions

$$V_0(0) = V_0(a) = 0, \tag{17a}$$

$$B_0(0) = B_0(a) = 0, \tag{17b}$$

and

$$\nabla^2 V_1 + M\frac{\partial B_1}{\partial x} = 0, \tag{18}$$

$$\nabla^2 B_1 + M\frac{\partial V_1}{\partial x} = 0, \tag{19}$$

with

$$V_1(0, y) = V_1(a, y) = 0, \qquad 0 \leqslant y < \infty, \tag{20a}$$

$$B_1(a, y) = 0, \qquad 0 \leqslant y < \infty, \tag{20b}$$

$$B_1(0, y) = 0, \qquad l < y < \infty, \tag{20c}$$

$$\frac{\partial B_1}{\partial x}(0, y) = -\frac{\partial B_0(0, y)}{\partial x}, \qquad 0 \leqslant y < l. \tag{20d}$$

On account of symmetry, we need to consider the solution only in the upper half of the xy-plane. The general solution of the system (15), (16) is given by

$$V_0(x) = A + Be^{Mx} + Ce^{-Mx},$$

$$B_0(x) = -\frac{x}{M} - (Be^{Mx} - Ce^{-Mx}) + D,$$

where A, B, C and D are constants. By making use of the boundry conditions (17) the primary flow is obtained as

$$V_0(x) = \frac{a}{2M \operatorname{sh}\left(\frac{Ma}{2}\right)}\left[\operatorname{ch}\left(\frac{Ma}{2}\right) - \operatorname{ch}\left[M\left(x - \frac{a}{2}\right)\right]\right], \tag{21}$$

$$B_0(x) = \frac{a}{2M \operatorname{sh}\left(\frac{Ma}{2}\right)} \operatorname{sh}\left[M\left(x - \frac{a}{2}\right)\right] - \frac{1}{M}\left(x - \frac{a}{2}\right), \tag{22}$$

where $\operatorname{sh}(x)$ and $\operatorname{ch}(x)$ are the sine hyperbolic and cosine hyperbolic functions, respectively.

To find the solution of the secondary flow, we define Fourier cosine transforms for V_1 and B_1:

$$\bar{V}_1(x, \alpha) = \int_0^\infty V_1(x, y) \cos(\alpha y)\, dy, \tag{23}$$

$$\bar{B}_1(x, \alpha) = \int_0^\infty B_1(x, y) \cos(\alpha y)\, dy. \tag{24}$$

Taking the Fourier cosine transform of equations (18) and (19) and the associated boundary conditions we obtain

$$\frac{d^2 \bar{V}_1}{dx^2} - \alpha^2 \bar{V}_1 + M \frac{d\bar{B}_1}{dx} = 0, \tag{25}$$

$$\frac{d^2 \bar{B}_1}{dx^2} - \alpha^2 \bar{B}_1 + M \frac{d\bar{V}_1}{dx} = 0, \tag{26}$$

and

$$\bar{V}_1(0, \alpha) = \bar{V}_1(a, \alpha) = 0, \qquad \bar{B}_1(a, \alpha) = 0. \tag{27}$$

Solving equations (25) and (26) subject to the boundary conditions (27) yields

$$\bar{V}_1(x, \alpha) = \frac{2A(\alpha)}{\operatorname{sh}(\rho_\alpha a)} \operatorname{sh}\left[\rho_\alpha (x - a)\right] \operatorname{sh}\left(\frac{Mx}{2}\right), \tag{28}$$

$$\bar{B}_0(x, \alpha) = \frac{-2A(\alpha)}{\operatorname{sh}(\rho_\alpha a)} \operatorname{sh}\left[\rho_\alpha (x - a)\right] \operatorname{ch}\left(\frac{Mx}{2}\right), \tag{29}$$

where

$$\rho_\alpha = (M^2/4 + \alpha^2)^{1/2}. \tag{30}$$

Inverting equations (28) and (29) and making use of the remaining boundary conditions (20c) and (20d), we obtain the following dual integral equations for $A(\alpha)$:

$$\int_0^\infty A(\alpha) \cos(y\alpha)\, d\alpha = 0, \qquad l < y < \infty, \tag{31}$$

$$\int_0^\infty \rho_\alpha A(\alpha) \operatorname{cth}(\rho_\alpha a) \cos(y\alpha)\, d\alpha = C, \qquad 0 \leqslant y < l, \tag{32}$$

where $\operatorname{cth}(x)$ is cotangent hyperbolic function and

$$C = \frac{\pi}{4}\left(\frac{a}{2} - \frac{1}{M} - \frac{a}{1 - e^{Ma}}\right). \tag{33}$$

Choosing the integral representation for $A(\alpha)$

$$A(\alpha) = \int_0^l f(t) J_0(\alpha t)\, dt, \tag{34}$$

and noting that equation (31) is automatically satisfied on account of the identity[19]

$$\int_0^\infty J_0(at)\cos(bt)\,dt = H(a-b)/\sqrt{(a^2-b^2)}, \tag{35}$$

where $J_0(x)$ and $H(x)$ are the Bessel function of the first kind of order zero, and the Heaviside function, respectively, equation (32) transforms to Abel's equation

$$\int_0^y f(t)/\sqrt{(y^2-t^2)}\,dt = p(y), \tag{36}$$

with

$$p(y) = Cy + \int_0^l f(t)\int_0^\infty \left[1 - \frac{\rho_\alpha}{\alpha}\mathrm{cth}(\rho_\alpha a)\right] J_0(\alpha t)\sin(y\alpha)\,d\alpha\,dt. \tag{37}$$

In obtaining equation (36), use was made of another identity

$$\int_0^\infty J_0(at)\sin(bt)\,dt = H(b-a)/\sqrt{(b^2-a^2)}. \tag{38}$$

The solution of (36) is well known (see, for example, Reference 18). It is given by

$$f(t) = \frac{2}{\pi}\frac{d}{dt}\int_0^t \frac{yp(y)}{\sqrt{(t^2-y^2)}}\,dy. \tag{39}$$

Substituting for $p(y)$ from equation (37) and making use of integral representations of Bessel functions, we finally arrive at the Fredholm integral equation of the second kind for $f(t)$:

$$f(t) + \int_0^l K(x,t)f(x)\,dx = Ct, \tag{40}$$

where

$$K(x,t) = \int_0^\infty \alpha t\left[\frac{\rho_\alpha}{\alpha}\mathrm{cth}(\rho_\alpha a) - 1\right] J_0(\alpha t)J_0(\alpha x)\,d\alpha. \tag{41}$$

At the time of writing, no analytical method is known to solve equation (40). It must, therefore, be solved numerically. There are a few advantages in putting the partial differential equations governing the flow in the form (40). First, we have been able to isolate the singularities at the junctions of insulating and conducting boundaries. Secondly, an integral equation is relatively easier to handle numerically than a set of partial differential equations. Thirdly, the system of linear algebraic equations resulting from discretization of the Fredholm integral equation of the second kind is diagonally dominant—theoretically at any rate—and is therefore guaranteed to yield a numerical solution. In practice, however, there are numerous computational considerations which must be taken into account, before attempting to solve equation (40) numerically.

COMPUTATIONAL CONSIDERATIONS

There are two main sources of possible trouble that we may encounter in obtaining the numerical solution of the Fredholm integral equation (40). First of all, we note that the kernel $K(x,t)$ in that equation, though convergent theoretically, has very poor convergence for computational purposes. Next, we observe that for large values of M, the kernel is of order M. This necessitates an extremely large number of mesh points in the discretization scheme. Since the coefficient matrix for

the integral equation is dense, it sets implementation limits on the size of the matrix, which means that we cannot go beyond certain values of M. This is really a limitation of computer memory and time and is not a drawback of the technique chosen in this paper.

Since we are primarily concerned with the MHD flow at intermediate to high values of Hartmann numbers ($10 \leqslant M \leqslant 200$) it is reasonable to approximate $\mathrm{c\,th}(\rho_\alpha a)$ in equation (41) by 1. With this approximation and the identity.[20]

$$J_0(\alpha t)J_0(\alpha x) = \frac{1}{\pi}\int_0^\pi J_0(\alpha(t^2 + x^2 - 2tx\cos\theta)^{1/2})\,\mathrm{d}\theta,$$

the kernel $K(x, t)$ can be transformed to a much more computationally efficient form by means of an identity (see Appendix I). We can rewrite equation (41) as

$$K(x,t) = \frac{M^2 t}{8\pi}\int_0^\pi [I_0(Mr/4)K_0(Mr/4) + I_1(Mr/4)K_1(Mr/4)]\,\mathrm{d}\theta, \tag{42}$$

where

$$r^2 = t^2 + x^2 - 2tx\cos\theta$$

and I_0, I_1, K_0 and K_1 are the modified Bessel functions of the first and second kinds and of order zero and one, respectively. It is to be noted that the kernel is now in a more easily computable form.

To solve the Fredholm integral equation (40), we replace the integrals by numerical quadratures based on Gauss's formula, and a system of algebraic equations is obtained for the unknown function f in the of representation $A(\alpha)$ (equation (34)). By virtue of the equation for $A(\alpha)$, the value of the function f can be substituted back in $\bar{V}_1(x, \alpha)$ and $\bar{B}_1(x, \alpha)$ (equations (28) and (29)) and then the secondary flow $V_1(x, y)$, $B_1(x, y)$ for the infinite channel problem can be found as

$$V_1(x,y) = \frac{4}{\pi}\mathrm{sh}\left(\frac{Mx}{2}\right)\int_0^l f(t)\int_0^\infty \frac{\mathrm{sh}[\rho_\alpha(x-a)]}{\mathrm{sh}(\rho_\alpha a)}J_0(\alpha t)\cos(y\alpha)\,\mathrm{d}\alpha\,\mathrm{d}t, \tag{43}$$

$$B_1(x,y) = -\frac{4}{\pi}\mathrm{ch}\left(\frac{Mx}{2}\right)\int_0^l f(t)\int_0^\infty \frac{\mathrm{sh}[\rho_\alpha(x-a)]}{\mathrm{sh}(\rho_\alpha a)}J_0(\alpha t)\cos(y\alpha)\,\mathrm{d}\alpha\,\mathrm{d}t. \tag{44}$$

The term $\mathrm{sh}[\rho_\alpha(x-a)]/\mathrm{sh}(\rho_\alpha a)$ can be approximated by $\mathrm{e}^{-\rho_\alpha(2a-x)} - \mathrm{e}^{-\rho_\alpha x}$ for large M, so $V_1(x, y)$, $B_1(x, y)$ can be transformed to the following forms (see Appendix II):

$$V_1(x,y) = \frac{2M}{\pi^2}\mathrm{sh}\left(\frac{Mx}{2}\right)g(x,y), \tag{45}$$

$$B_1(x,y) = -\frac{2M}{\pi^2}\mathrm{ch}\left(\frac{Mx}{2}\right)g(x,y), \tag{46}$$

where

$$g(x,y) = \int_0^l f(t)\int_0^\pi \left[(2a-x)\frac{K_1\left(\frac{M}{2}\sqrt{[(t\cos\theta + y)^2 + (2a-x)^2]}\right)}{\sqrt{[(t\cos + y)^2 + (2a-x)^2]}}\right.$$
$$\left. - x\frac{K_1\left(\frac{M}{2}\sqrt{[(t\cos\theta + y)^2 + x^2]}\right)}{\sqrt{[(t\cos\theta + y)^2 + x^2]}}\right]\mathrm{d}\theta\,\mathrm{d}t. \tag{47}$$

By adding the primary solution V_0, B_0 to the secondary solution V_1, B_1, one can find the velocity $V(x, y)$ and the induced magnetic field $B(x, y)$ for the infinite channel problem.

The magnetic field on the conducting portion of the mixed boundary can be found directly from substitution of $A(\alpha)$ in $B_1(x, y)$. Simplifying we obtain

$$B(0, y) = \frac{4}{\pi} \int_y^l \frac{f(t)}{\sqrt{(t^2 - y^2)}} \mathrm{d}t, \qquad 0 \leqslant y < l, \tag{48}$$

which can be further transformed to the form

$$B(0, y) = \frac{4}{\pi} \int_0^{\operatorname{arcch}(l/y)} f(y \operatorname{ch}\theta) \, \mathrm{d}\theta. \tag{49}$$

The function f was interpolated with Gauss–Legendre abscissae at the points $y \operatorname{ch}\theta$, using Lagrange interpolation.

NUMERICAL RESULTS AND DISCUSSIONS

The velocity field and the induced magnetic field were calculated in the region $0 \leqslant x \leqslant a(= 1) \cap 0 \leqslant y \leqslant 2$ using appropriate step sizes. For the velocity field near $y = 0$, finer meshes were chosen to obtain the desired accuracy in the results. Calculations have been carried out for Hartmann numbers 10, 20, 50, 100 and 200.

The system of linear algebraic equations arising from discretizing equation (40) was solved by calling the matrix solver LEQT2F on Honeywell Multics at the University of Calgary, Canada. This subroutine performs Gaussian elimination with pivoting and improved the results iteratively.

The equal velocity lines and current lines (equal induced magnetic field lines) were obtained by using the SURFACE II contour package, which uses linear interpolation. The non-smoothness of some of the curves can be explained as due to it.

In Figures 2–4 equal velocity lines have been drawn for $l = 0{\cdot}3$ and for $M = 20$, 50, 200, respectively. We notice from these graphs that as Hartmann number M is increased, there is a

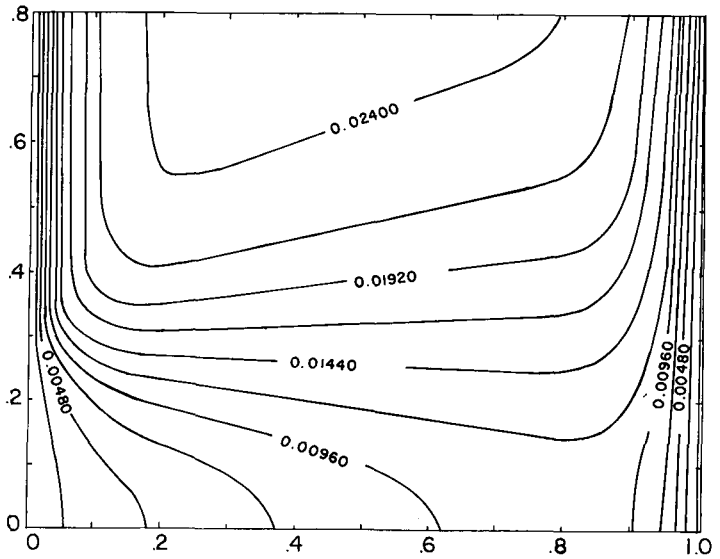

Figure 2. Velocity lines for $M = 20$, $l = 0{\cdot}3$

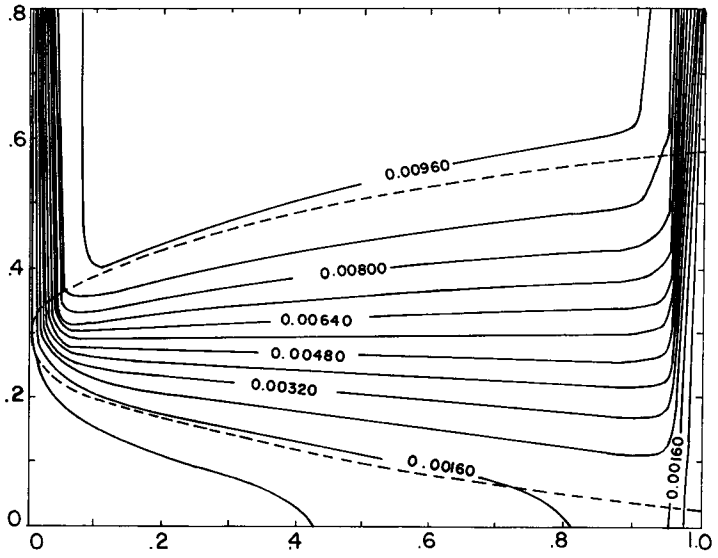

Figure 3. Velocity lines for $M = 50$, $l = 0{\cdot}3$

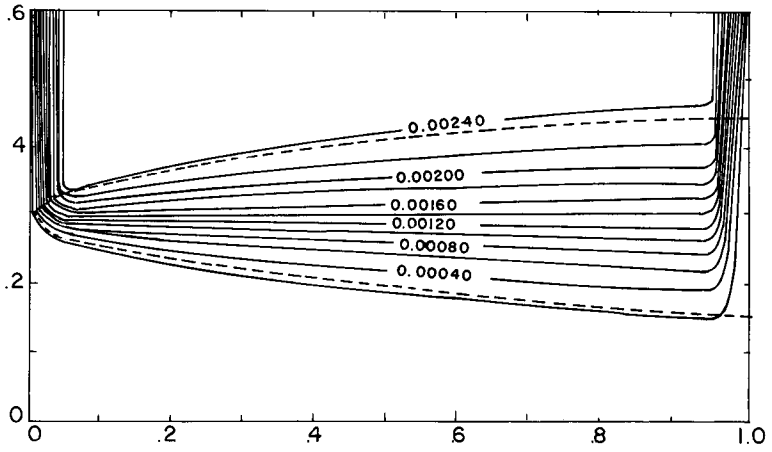

Figure 4. Velocity lines for $M = 200$, $l = 0{\cdot}3$

formation of boundary layers near the non-conducting parts of the boundaries. In the core of the channel, for $|y| > l$ the velocity is almost stationary and is equal to the maximum value of V, whereas the region $|y| < l$ is mostly stagnant for large M.

In Figures 5–7 current lines have been drawn for $l = 0{\cdot}3$ and various values of M. Again we can notice the formation of boundary layers for increasing values of M. However, there is an interesting pattern of current lines. We can separate these lines by a value of B, say B_{crit}, which depends on M and l. For $B > B_{crit}$ all current lines start from the conducting part of the boundary and form closed loops. For every positive value of B less than B_{crit} there are three current lines, two of which start from the conducting part and symmetrically move with the channel (these current lines form the Hartmann layer at the mixed boundary). The remaining current line spans the entire length of the channel to the right of the region of the loops of the current lines characterized by $B > B_{crit}$. Lastly,

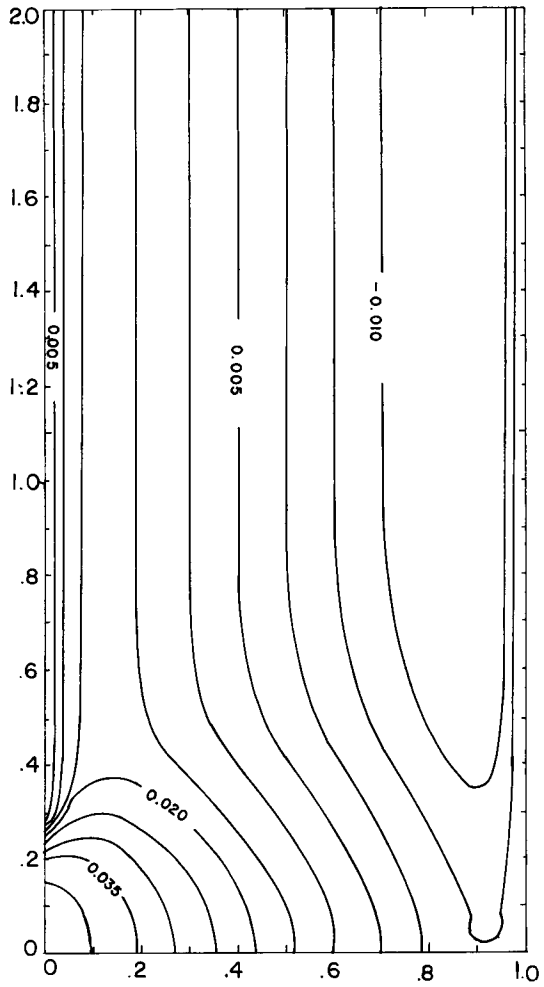

Figure 5. Magnetic field lines for $M = 20$, $l = 0{\cdot}3$

for negative values of B, the current lines form the loops which turn back nearly at a distance equal to the conducting part of the boundary from the central line. These current lines form the Hartmann layer at the non-conducting boundary.

We also note from these Figures that there is a parabolic boundary layer with thickness of order $M^{-1/2}$ at the point of discontinuity on the boundaries. This boundary layer is shown using dashed lines.

The length of the conducting part l was varied keeping M fixed, and the results are shown in Figures 8–11. As l increases, the same kind of behaviour for equal velocity lines, as outlined above, by increasing M, is exhibited. The effect of increasing l is that more equal velocity lines are forced to turn away from the central line, and this leads to further demarcation of the separate regions for current lines.

Experiments on the flow of conducting liquids (e.g. mercury, liquid sodium) normally refer to channels of circular or rectangular cross-section. Flow through the latter may be expected to approximate the flow between parallel planes if one side of the rectangle is large compared with the

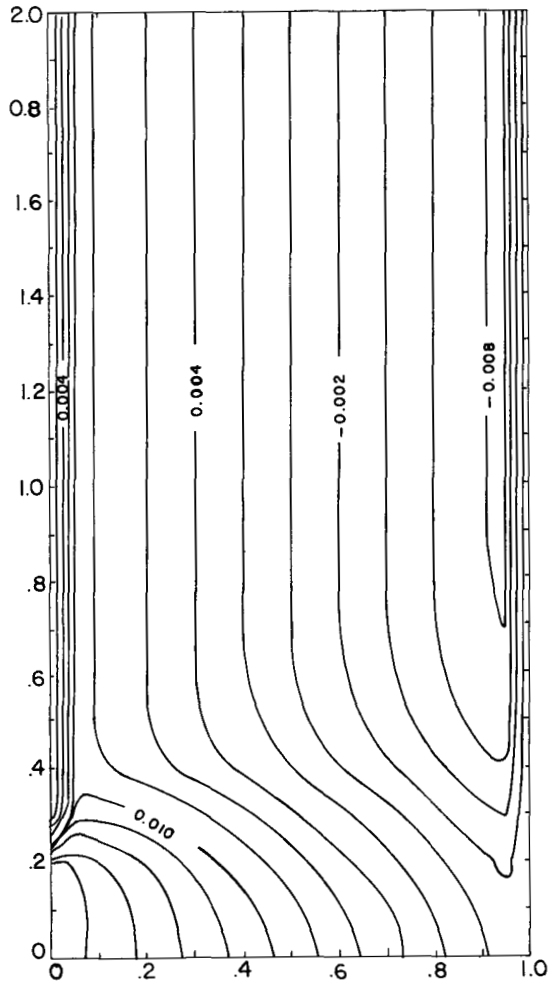

Figure 6. Magnetic field lines for $M = 50$, $l = 0{\cdot}3$

other, the applied magnetic field being perpendicular to the long side. Assuming a constant value of pressure gradient and taking one of the long sides to be partly insulated and partly conducting, one can set up an illustrative problem relevant to this analysis.

For example, if the liquid is mercury at 20°C, the corresponding physical constants are,[21] $\rho = 13{,}550\,\text{kg/m}^3$ (density), $\mu = 0{\cdot}00155\,\text{kg/m s}$, $\sigma = 1{\cdot}05 \times 10^6\,\text{mho/m}$ and $\mu_e = 11 \times 10^{-7}\,\text{mho/s}$ ins MKS units. We may choose the characteristic length $L_0 = 0{\cdot}03\,\text{m} = 3\,\text{cm}$ and the pressure gradient $\partial p/\partial z = -0{\cdot}25\,\text{kg/m}^2\,\text{s}^2$. The conversions to actual flow velocities and magnetic fields with units are performed through equations (7), (8) and (9) for $M = 20$, 50 and 200, and also the Reynolds number Re is checked in each case, since the flow is laminar. The new results are shown, with units, in Table I. We note from these figures that as M increases V_z is decreasing and B_z is small compared with B_0.

On each Figure, we have chosen the maximum equal velocity line and one current line to indicate the actual values of flow velocity and induced magnetic field with their units on these lines, respectively.

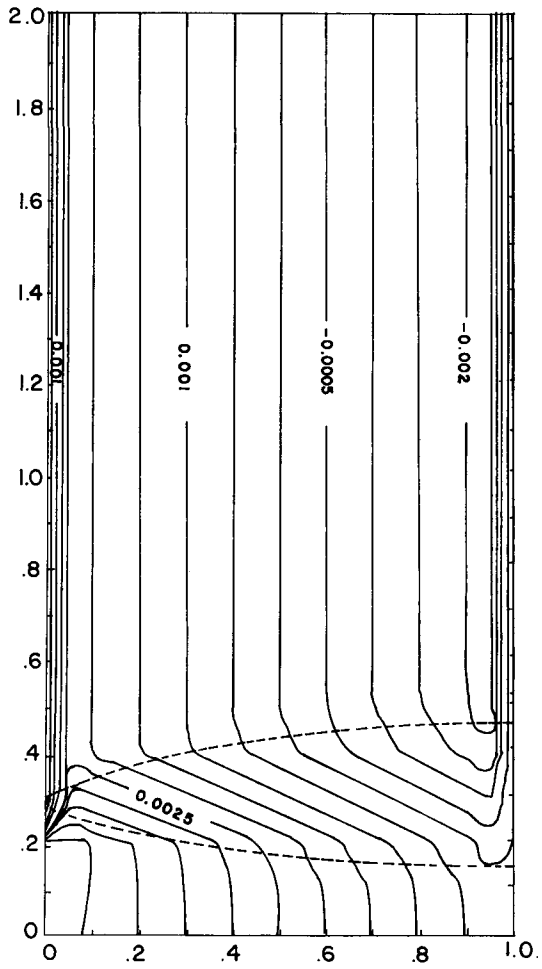

Figure 7. Magnetic field lines for $M = 200$, $l = 0{\cdot}3$

Table I

$M = 20$ $V_{max} = 0{\cdot}024$ $B = 0{\cdot}02$	$M = 50$ $V_{max} = 0{\cdot}0096$ $B = 0{\cdot}01$	$M = 200$ $V_{max} = 0{\cdot}0024$ $B = 0{\cdot}0025$	$M = 10$ $V_{max} = 0{\cdot}048$ $B = 0{\cdot}03$ and $B = 0{\cdot}007$
Chosen from Figures 2 and 5	Chosen from Figures 3 and 6	Chosen from Figures 4 and 7	Chosen from Figures 8–11
$v_0 = 14{\cdot}5$ cm/s $Re = 912$ $V_z = 0{\cdot}348$ cm/s $B_0 = 255$ gauss $B_z = 1{\cdot}2856$ $\times 10^{-3}$ gauss	$v_0 = 14{\cdot}5$ cm/s $Re = 365$ $V_z = 0{\cdot}139$ cm/s $B_0 = 637$ gauss $B_z = 0{\cdot}6428$ $\times 10^{-3}$ gauss	$v_0 = 14{\cdot}5$ cm/s $Re = 91{\cdot}265$ $V_z = 0{\cdot}0348$ cm/s $B_0 = 2555$ gauss $B_z = 0{\cdot}1607$ $\times 10^{-3}$ gauss	$v_0 = 14{\cdot}5$ cm/s $Re = 1825{\cdot}3$ $V_z = 0{\cdot}696$ cm/s $B_0 = 129$ gauss $B_z = 1{\cdot}9$ $\times 10^{-3}$ gauss for $B = 0{\cdot}03$ and $B_z = 4{\cdot}49 \times 10^{-3}$ for $B = 0{\cdot}07$

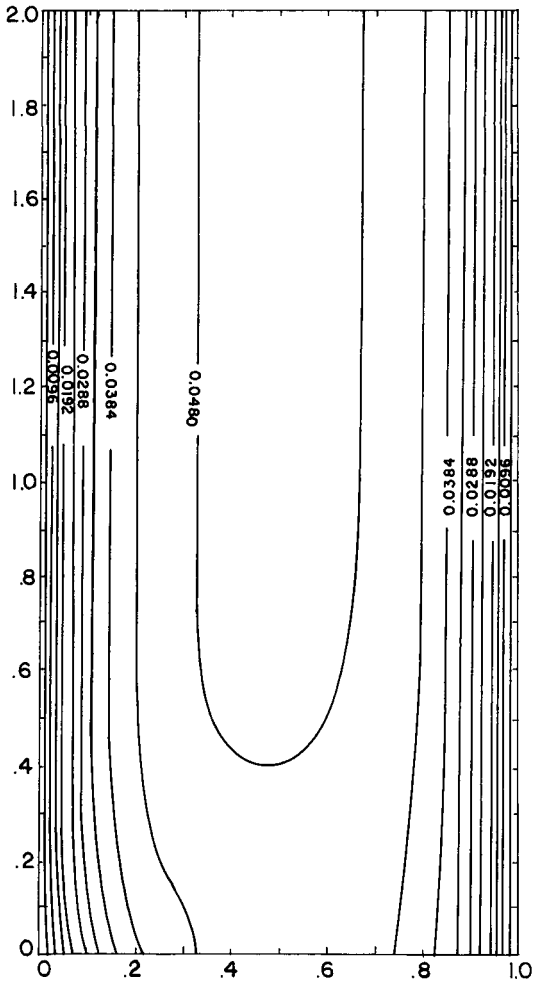

Figure 8. Velocity lines for $M = 10$, $l = 0{\cdot}1$

APPENDIX I

Consider[19]

$$J = \int_0^\infty (\beta^2 + x^2)^{-1/2} e^{-\alpha(\beta^2+x^2)^{1/2}} J_0(\gamma x)\,dx = I_0(\beta p_-) K_0(\beta p_+), \tag{50}$$

where

$$p_- = \tfrac{1}{2}[(\alpha^2+\gamma^2)^{1/2} - \alpha],$$
$$p_+ = \tfrac{1}{2}[(\alpha^2+\gamma^2)^{1/2} + \alpha].$$

So,

$$\frac{dp_-}{d\alpha} = -\frac{p_-}{\sqrt{(\alpha^2+\gamma^2)}}, \quad \frac{dp_+}{d\alpha} = \frac{p_+}{\sqrt{(\alpha^2+\gamma^2)}}. \tag{51}$$

Taking the derivative of J with respect to α

$$\frac{dJ}{d\alpha} = -\int_0^\infty e^{-\alpha(\beta^2+x^2)^{1/2}} J_0(\gamma x)\,dx$$

$$= -\frac{\beta}{\sqrt{\alpha^2+\gamma^2}}\{I_0(\beta p_-)p_+ K_1(\beta p_+) + K_0(\beta p_+)p_- I_1(\beta p_-)\}.$$

Taking the second derivative of J with respect to α,

$$\frac{d^2J}{d\alpha^2} = \int_0^\infty (\beta^2+x^2)^{1/2} e^{-\alpha(\beta^2+x^2)^{1/2}} J_0(\gamma x)\,dx$$

$$= \frac{\alpha\beta}{(\alpha^2+\gamma^2)^{3/2}}\{p_+ I_0(\beta p_-)K_1(\beta p_+) + p_- I_1(\beta p_-)K_0(\beta p_+)\}$$

$$+ \frac{\beta^2}{\alpha^2+\gamma^2}\{(p_+^2+p_-^2)I_0(\beta p_-)K_0(\beta p_+)$$

$$+ 2p_+ p_- I_1(\beta p_-)K_1(\beta p_+)\}. \tag{52}$$

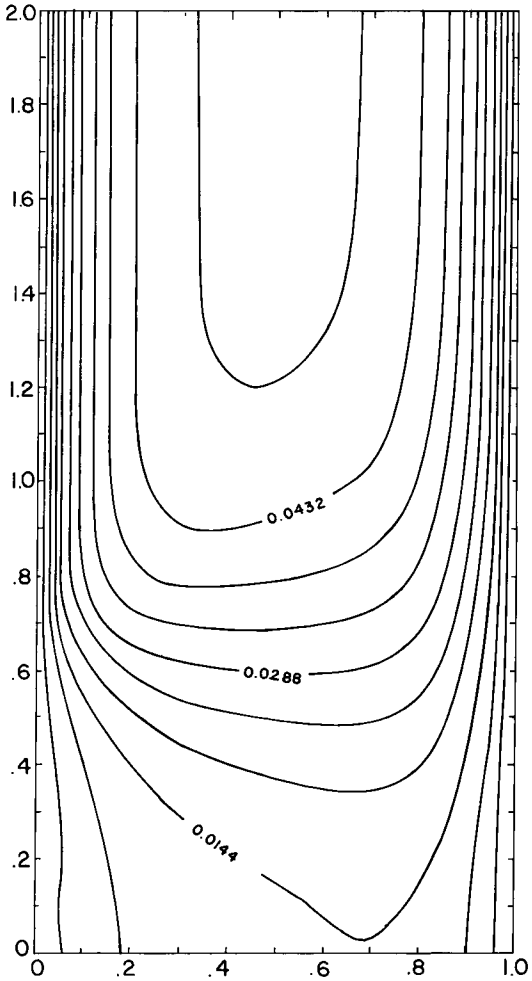

Figure 9. Velocity lines for $M = 10$, $l = 0{\cdot}7$

Letting $\beta \to 0$ in (52), we obtain

$$\int_0^\infty x e^{-\alpha x} J_0(\gamma x)\,dx = \frac{\alpha}{(\alpha^2+\gamma^2)^{3/2}}. \tag{53}$$

Then subtracting (53) from (52) and letting $\alpha \to 0$, we obtain

$$\int_0^\infty [(\beta^2+x^2)^{1/2} - x] J_0(\gamma x)\,dx = \tfrac{1}{2}\beta^2 [I_0(\tfrac{1}{2}\beta\gamma)K_0(\tfrac{1}{2}\beta\gamma) + I_1(\tfrac{1}{2}\beta\gamma)K_1(\tfrac{1}{2}\beta\gamma)]. \tag{54}$$

APPENDIX II

Consider the integral

$$R = \int_0^\infty e^{-k\sqrt{(u^2+\alpha^2)}} \cos(y\alpha) J_0(\alpha t)\,d\alpha. \tag{55}$$

Since

$$J_0(z) = \frac{1}{\pi}\int_0^\pi \cos(z\cos\theta)\,d\theta$$

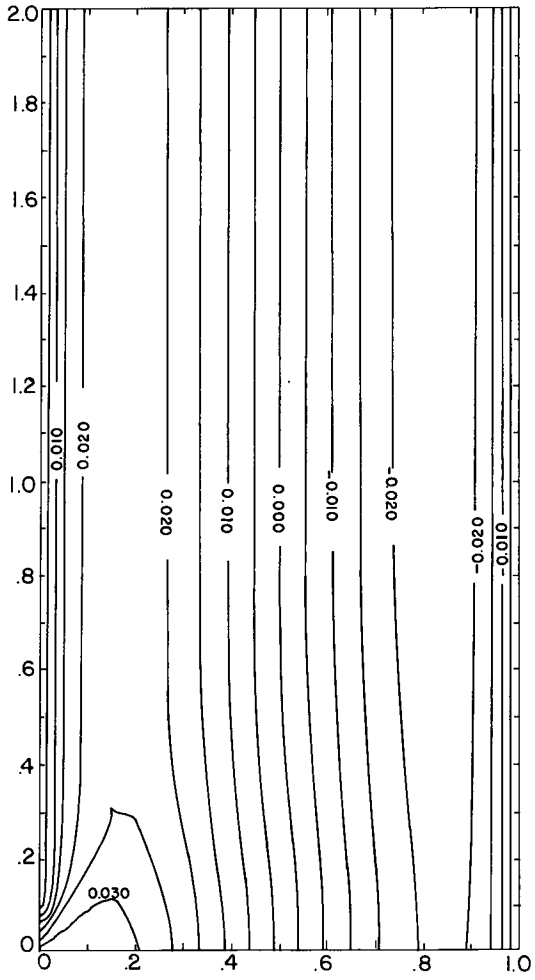

Figure 10. Magnetic field lines for $M = 10$, $l = 0{\cdot}1$

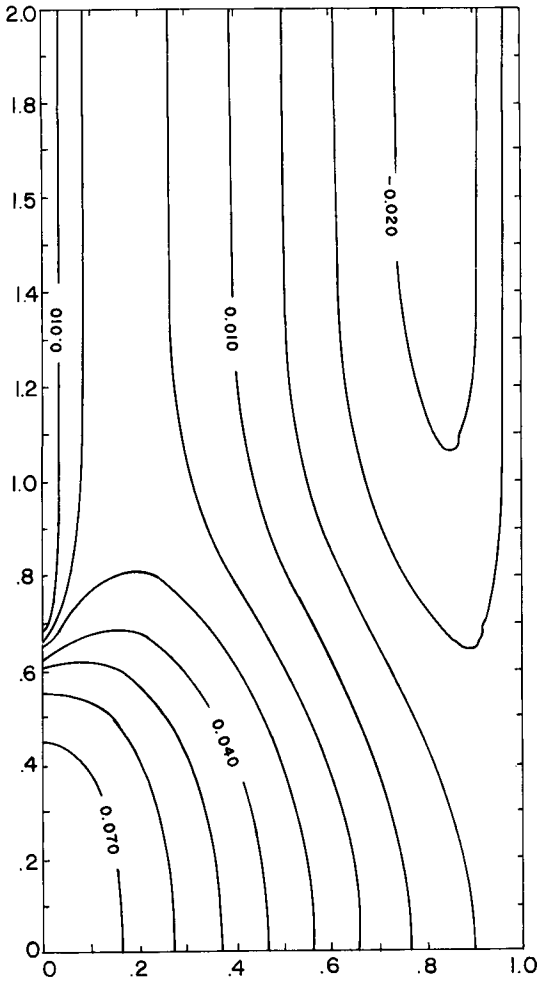

Figure 11. Magnetic field lines for $M = 10$, $l = 0{\cdot}7$

the integral (55) can be written as

$$R = \frac{1}{\pi}\int_0^\infty e^{-k\sqrt{(u^2+\alpha^2)}}\int_0^\pi \cos(\alpha t\cos\theta)\cos(y\alpha)\,d\theta\,d\alpha,$$

$$= \frac{1}{2\pi}\int_0^\infty e^{-k\sqrt{(u^2+\alpha^2)}}\int_0^\pi [\cos\alpha(t\cos\theta + y) + \cos\alpha(t\cos\theta - y)]\,d\theta\,d\alpha,$$

$$= \frac{1}{2\pi}\int_0^\pi \left[\int_0^\infty e^{-k\sqrt{(u^2+\alpha^2)}}\cos\alpha(t\cos\theta + y)\,d\alpha + \int_0^\infty e^{-k\sqrt{(u^2+\alpha^2)}}\cos\alpha(t\cos\theta - y)\,d\alpha\right] d\theta. \tag{56}$$

For the evaluation of the infinite integrals above we make use of the identity[17]

$$\int_0^\infty e^{-\beta\sqrt{(\gamma^2+x^2)}}\cos(ax)\frac{dx}{\sqrt{(\gamma^2+x^2)}} = K_0[(\gamma\sqrt{(a^2+\beta^2)}]. \tag{57}$$

By taking the derivative of (57) with respect to β we arrive at

$$\int_0^\infty e^{-\beta\sqrt{(\gamma^2+x^2)}}\cos(ax)\,dx = K_1[(\gamma\sqrt{(a^2+\beta^2)}]\frac{\gamma\beta}{\sqrt{(a^2+\beta^2)}}. \tag{58}$$

Now, substituting (58) back into (56) we obtain

$$R = \frac{uk}{2\pi}\int_0^\pi \left[\frac{K_1\{u\sqrt{[(t\cos\theta+y)^2+k^2]}\}}{\sqrt{[(t\cos\theta+y)^2+k^2]}} + \frac{K_1\{u\sqrt{[(t\cos\theta-y)^2+k^2]}\}}{\sqrt{[(t\cos\theta-y)^2+k^2]}}\right]d\theta$$

$$= \frac{uk}{\pi}\int_0^\pi \frac{K_1\{u\sqrt{[(t\cos\theta+y)^2+k^2]}\}}{\sqrt{[(t\cos\theta+y)^2+k^2]}}\,d\theta.$$

Therefore,

$$\int_0^\infty e^{-k\sqrt{(u^2+\alpha^2)}}\cos(y\alpha)J_0(\alpha t)\,d\alpha = \frac{uk}{\pi}\int_0^\pi \frac{K_1\{u\sqrt{[(t\cos\theta+y)^2+k^2]}\}}{\sqrt{[(t\cos\theta+y)^2+k^2]}}\,d\theta. \tag{59}$$

REFERENCES

1. J. A. Shercliff, 'Steady motion of conducting fluids in pipes under transverse magnetic fields', *Proc. Camb. Phil. Soc.*, **49**, 136–144 (1953).
2. C. C. Chang and T. S. Lundgren, 'Duct flow in MHD', *Z. Angew. Math. Phys.*, **12**, 100–114 (1961).
3. R. R. Gold, 'Magnetohydrodynamic pipe flow I', *J. Fluid Mech.*, **13**, 505 (1962).
4. J. C. R. Hunt, 'MHD flow in rectangular ducts', *J. Fluid Mech.*, **21**, (4), 577–590 (1965).
5. G. A. Grinberg, 'On steady flow of a conducting fluid in a rectangular tube with two nonconducting walls, and two conducting ones parallel to an external magnetic field', *PMM*, **25**, (6), 1024–1034 (1961).
6. G. A. Grinberg, 'On some types of flow of a conducting fluid in pipes of rectangular cross-section, placed in a magnetic field', *PMM*, **26**, (1), 80–87 (1962).
7. J. C. R. Hunt and K. Stewartson, 'MHD flow in a rectangular duct II', *J. Fluid Mech.*, **23**, (3), 563–581 (1965).
8. D. Chiang and T. Lundgren, 'MHD flow in a rectangular duct with perfectly conducting electrodes', *Z. Angew. Math. Phys.*, **18**, 92–105 (1967).
9. B. Singh and P. K. Agarwal, 'Numerical solution of a singular integral equation appearing in MHD', *Z. Angew. Math. Phys.*, **35**, 760–769 (1984).
10. J. C. R. Hunt and W. E. Williams, 'Some electrically driven flows in MHD', *J. Fluid Mech.*, **31**, 705–722 (1968).
11. N. C. Wenger, 'A variational principle for magnetohydrodynamic channel flow', *J. Fluid Mech.*, **43**, (1), 211–224 (1970).
12. S. Y. Wu, 'Unsteady MHD duct flow by finite element method', *Int. J. numer. method eng.*, **6**, 3 (1973).
13. B. Singh and J. Lal, 'Finite element method in MHD channel flow problems', *Int. J. numer. methods eng.*, **18**, 1091–1111 (1982).
14. B. Singh and J. Lal, 'Quadratic finite elements in steady MHD channel flows with nonconducting walls', *Ind. J. Pure Appl. Math.*, **14**, 1473 (1983).
15. B. Singh and J. Lal, 'Finite element method for unsteady MHD flow through pipes with arbitrary wall conductivity', *Int. J. numer. methods fluids*, **4**, 291–302 (1984).
16. L. Dragos, *Magnetofluid Dynamics*, Abacus Press, 1975.
17. I. S. Gradshteyn and I. M. Ryzhik, *Tables of Integrals, Series and Products*, Academic Press Inc., New York and London, 1965.
18. I. N. Sneddon, *Mixed Boundary Value Problems in Potential Theory*, North-Holland, Wiley, New York, 1966.
19. F. Oberhettinger, *Tables of Bessel Transforms*, Springer-Verlag, 1972.
20. G. Eason, B. Nobel and I. N. Sneddon, 'On certain integrals of Lipschitz–Hankel type involving products of Bessel functions', *Phil. Trans. Roy. Soc., Series A*, **247**, 529–551 (1955).
21. K. R. Cramer and Shih-I Pai, *Magnetofluid Dynamics for Engineers and Applied Physicists*, McGraw-Hill, 1973.